General Disclaimer

One or more of the Following Statements may affect this Document

- This document has been reproduced from the best copy furnished by the organizational source. It is being released in the interest of making available as much information as possible.

- This document may contain data, which exceeds the sheet parameters. It was furnished in this condition by the organizational source and is the best copy available.

- This document may contain tone-on-tone or color graphs, charts and/or pictures, which have been reproduced in black and white.

- This document is paginated as submitted by the original source.

- Portions of this document are not fully legible due to the historical nature of some of the material. However, it is the best reproduction available from the original submission.

Produced by the NASA Center for Aerospace Information (CASI)

BOLT BERANEK · AND NEWMAN INC

CONSULTING · DEVELOPMENT · RESEARCH

Report No. 2100
Job No. 115042

ACOUSTICAL EVALUATION OF THE

NASA LANGLEY FULL-SCALE WIND TUNNEL

By István L. Vér
Charles I. Malme
Eugene B. Meyer

Contract No. NAS1-9559

15 January 1971

Submitted to:

H. H. Hubbard
NASA, Langley Research Center
Building 1195, Mail Stop 139
Hampton, Virginia 23365

CAMBRIDGE   NEW YORK   CHICAGO   LOS ANGELES

ACOUSTICAL EVALUATION OF THE

NASA LANGLEY FULL-SCALE WIND TUNNEL

By István L. Vér
     Charles I. Malme
     Eugene B. Meyer

Contract No. NAS1-9559

15 January 1971

TABLE OF CONTENTS

List of Figures

References .

LIST OF FIGURES

I. SUMMARY

This report summarizes the acoustical measurements done by
BBN under Task Order No. 7 of the Master Agreement NAS1-9559
at the NASA Langley Research Center's Full Scale Wind Tunnel.
The purpose of these measurements was to supply NASA Langley
operating personnel with data indicating the types of acoustical
measurements which can be undertaken in the tunnel test section.
The series of measurements included:

1. Evaluation of the octave band ambient noise level in the
    test section with the tunnel fans stationary.

2. Evaluation of the octave band noise levels in the test
    section as a function of the air speed in three different
    locations in the tunnel test section.

3. Mapping of the sound field of an omnidirectional continuous
    broadband sound source of known power output.

4. Measurement of decay rate in the test section and in certain
    other locations in the tunnel.

An analysis of the measured data indicates that the test section
of the full scale wind tunnel has potential as an environment
for performing some types of acoustical measurements. The
validity of the test results will be dependent upon the type of
noise source to be investigated, (i.e. upon the acoustical power
output, radiation pattern frequency spectrum and dimensions of
the source) the distance from the source where measurements to
be taken and upon the air flow conditions. Accordingly, there
are practical limitations in acoustical testing which can be
performed and care should be exercised in planning experiments
in order to insure that the results are valid. As presently
constituted, the tunnel test section has an acoustical dis-
advantage. Because of the large tunnel openings which act as
completely absorbing surfaces while all the other boundaries are

hard, the sound absorption in the test section is very un-
evenly distributed. Accordingly, the reverberant sound field
in the test section is far from being diffuse. This non-
diffuse nature of the sound field manifests itself in un-
certainties in prediction and interpretation of the measured
data.

Adding sound absorbing treatment to certain interior surfaces
of the test section would increase the utility of the tunnel
by causing a corresponding increase of the radius within which
meaningful acoustical measurements can be performed. In
order to obtain a cost-effective improvement it is recommended
that quantity and location of the required sound absorbing
treatment should be determined experimentally utilizing a
small-scale acoustical model of the tunnel test section.

II. ACOUSTICAL ENVIRONMENT

The plan and elevation of the full-scale wind tunnel is shown
schematically in Fig. 1. The two 35 ft. diameter propellers
enclosed in the shroud force the air to circulate. The air
flow enters the nozzle upstream of the test section through
airfoil-shaped turning vanes. The air flow reaches the test
section through the 60 ft. x 30 ft. exit area of the nozzle
where the test object is mounted on a 21-1/4 ft. high platform.
The 31 ft. x 63 ft. entrance section of the shroud guides
the flow to the propeller

The tunnel was not designed to be used for acoustical measure-
ments. It does not contain any sound absorbing wall treatment
in the test section nor silencers in the path of air circulation
which would attenuate the fan noise before it can enter the
test section. Accordingly, the ambient noise of the tunnel
is high. The sound energy builds up a reverberant field to
a level where the energy loss provided by the sound trans-
mission loss and viscous loss of the partitions making up
the boundaries of the tunnel and the air absorption balance
the acoustical power output of the driving fans.

The acoustical environment of the test section is of particular
interest since NASA plans to carry out experimental research
on the sound generation by aerodynamic processes (i.e., vortex
noise of propellers). For such processes the presence of the
dc airflow may considerably influence the power output of
the source (e.g., by preventing one blade from cutting through
the vortex of the preceding blade).

The sound radiated by a test object builds up a complex sound
field in the test section. In order to prepare the reader
for the interpretation of the experimental results given in
the following sections of this report, it seems appropriate
at this point to first describe the sound field in this section
of the tunnel in qualitative terms.

Depending on their direction of propagation, the sound waves
radiated by the test object either 1) hit one of the solid
boundaries of the test section or 2) enter the shroud or the
nozzle. The sound energy carried by the latter waves can be
considered as practically lost for the test section (it does
not contribute to the buildup of the reverberant sound field
in the test section). Since these two acoustically "open
windows" make up approximately 7% of the total wall surface
area (and an even larger percentage of the solid angle these
areas project on the surface of a sphere placed at the location
of the source) this energy loss, especially if the directivity
of the radiation has a maximum in either the direction of nozzle
or the shroud opening, can be considerable. Since one usually
does not know the exact directivity pattern of sound radiation
of the test object, one cannot determine the corresponding
fraction of the power output of the source which immediately
escapes through these openings. Thus, it is expected that
one will not find a simple relation between the space average
sound pressure in the test section and the total power output
of the source as would be expected in well-behaved reverberation
chambers with evenly distributed absorption.

Most of those sound waves (rays) which were initially directed
toward the solid boundaries of the test section will reach
the nozzle or shroud opening after a certain number of reflec-
tions. It is expected that for an initial period of time

4

the energy loss through those waves exiting through the nozzle
and shroud opening remains larger than the energy loss suffered
by the waves when reflected from the room boundaries and that
these waves will control the initial slope of the decay rate
curve.

After almost all of the energy carried by those waves having
a component in the direction of the nozzle-shroud axis is
lost, the sound field in the test section becomes dominated
by those remaining waves running in the two directions per-
pendicular to the shroud-nozzle axis. The decay rate of
these waves (i.e., the second slope of the decay curve) is
mostly controlled by the average absorption coefficient of
the respective partitions perpendicular to these axes. The
sound field in the test section at this time is very far from
being a true three-dimensional, diffuse sound field, namely,
the waves with components in the nozzle-shroud axis are almost
completely missing.

In summary, the particular distribution of the sound absorbing
surfaces across the boundaries of the tunnel test section
(which is necessary to provide the required dc flow) is
expected to manifest itself in non-exponential decay rates
of sound and in a directional distribution of the sound
waves which do not result in a diffuse reverberant sound
field. Accordingly, the formulas to calculate the total
sound power output of a source from the space average sound
pressure level in the reverberant field and from the measured
reverberation time, which are based on the assumptions of
a truely diffuse sound field are not applicable for the tunnel
test section.

The total sound power output of an unknown source in this
environment can be calculated only by integrating the intensity
of the direct sound field over all directions on an imaginary
surface enclosing the source.

III. AMBIENT NOISE IN THE TEST SECTION

The ambient noise in the test section of the full scale
wind tunnel is the sum of the noise of interior sources
(such as fire compressor, air conditioning equipment, noise
of pressure reducing valves, etc.), the noise intruding from
the outside (e.g., takeoff, landing or runnup of aircraft
from the nearby airstrip or occasional construction noise),
and the aerodynamic noise generated by the tunnel fans and
by the airflow impinging upon solid surfaces.

A. Ambient Noise with the Tunnel Stationary

The lowest ambient noise is obtained when the tunnel is sta-
tionary and there are no takeoffs, landing or runup operations
at the nearby air force base. Figure 2 shows the measured
octave band ambient noise spectrum for this situation with
the air conditioning and ventilating system shut off. Measuring
nearly the same ambient noise level at locations A, B and C
(see Fig. 1) indicated that the ambient noise level in the
test section has an even spatial distribution. Except for
the noise of the intermittently operating fire compressor,
which reaches the test section through the structureborne
path, we were not able to identify any significant noise
sources. Accordingly, for a stationary tunnel the octave
band ambient noise level as plotted in Fig. 2 may be regarded
as practically the lowest achievable in the tunnel test
section. Because of the large volume of test section, one
would, however, expect some variation of the ambient noise
at high frequencies (above 1 kHz) due to the change of humidity
and temperature which affects the air absorption.

6

B. Ambient Noise with the Tunnel Operational

If the tunnel is operational the ambient noise in the test
section increases due to the vortex noise created at the tip
of the fan blades. The acoustical power output of a dipole-
type aerodynamic noise source, such as created by the interaction
of vortices with solid boundaries, is proportional to the
sixth power of the relative velocity between the airstream
and the solid surface. Therefore, it is reasonable to expect
that the ambient of the tunnel is controlled by the noise
generated at and near the tip of the fan blades, where the
relative velocity is much larger than at any other section of
the tunnel (e.g. at turning vanes, nozzle, etc.). Observations
and noise measurements made near the turning vanes indeed
indicated that the sound power generated by the turning vanes
is small compared with the sound power generated by the driving
fans. Accordingly, the tunnel fans may be regarded as the
dominant source of the ambient noise in the test section.

Figure 3 shows the octave band ambient sound pressure level
measured on the test platform (Position A) with the tunnel
speed as a parameter. As expected, the ambient noise increases
with increasing tunnel speed. Measurements of the ambient
noise at positions B and C agreed well with the noise measured
at Position A indicating that also for the operating tunnel
the ambient noise in the test section retains its nearly
even spatial distribution.

Since the general shape of the octave band ambient noise
levels vs. frequency curve was found to be very similar for
all tunnel speeds investigated, and we expected a sixth power

7

dependence for the sound power output vs. tunnel speed (and
accordingly also for the ambient noise level in the test
section), we attempted to normalize the octave band ambient
noise level as:

$$SPL_N(OCT) = SPL(OCT, U_{MPH}) - 60 \log_{10}(U_{MPH}) \qquad (1)$$

where $SPL_N(OCT)$ = normalized octave band ambient sound pressure
level given in Eq. 1

$SPL(OCT, U_{MPH})$ = octave band ambient sound pressure level in
dB re 0.0002 microbar measured for tunnel
speed U_{MPH}

U_{MPH} = tunnel speed normalized to one mile/hour

Figure 4 shows the range and average value of the normalized
octave band ambient sound pressure level as a function of
the octave band center frequency. The level range between
the two dotted lines contains all of the measured data for
Positions A, B and C and for tunnel speeds from 27 mph to
71 mph. In spite of the considerable speed range and the
spatial effects, the level range between the two dotted lines
remains relatively small indicating that not only the overall
sound power output of the tunnel fans but also the power in
each of the octave bands increases with the sixth power of
the tunnel speed. Accordingly, the octave band spectrum of
the ambient noise level in the test section can be predicted
for each tunnel speed by Eq. 2, namely:

$$SPL(OCT, U_{MPH}) = SPL_N(OCT) + 60 \log U_{MPH} \qquad (2)$$

where $SPL_N(OCT)$ = the curve drawn as a solid line in Fig. 4

U_{MPH} = tunnel speed normalized to one mile/hour

Because of the relatively small scatter of the data points around the solid curve in Fig. 4, a Strouhal number scaling was not attempted.

IV. SPATIAL DISTRIBUTION OF THE SOUND PRESSURE LEVEL IN THE TEST SECTION

If a sound source placed in a room is switched on, the radiated sound energy spreads spherically. The sound pressure level decreases by approximately 6 dB for each doubling of the distance between the observation point and the acoustical center of the source except for the immediate vicinity of the source in the so-called near field where the decrease can be much faster.

When the sound waves reach the boundaries of the room, they are partially reflected. These waves suffering multiple reflections on the room boundaries build up a reverberant field in the room which exhibits a spatially homogenous pattern for "well behaved" rooms. This reverberant sound field in the room builds up until it reaches such a level that sound energy lost during unit time through absorption at the room boundaries and through air absorption equals the sound power output of the source. If the sound field in the room is diffuse, the sound power incident on a unit surface area of the room boundary is given by:

$$W_{inc} = \frac{\overline{p^2_{rev}}}{4\rho_0 c_0} \qquad (3)$$

where $\overline{p^2}$ = space-time average sound pressure squared in the room

ρ_0 = density of air

c_0 = propagation speed of sound in air

The sound power dissipated by the total room boundary of
area S and average sound absorption coefficient $\bar{\alpha}$
and the power loss through air absorption must be equal
to the power output of the source, W_0. This yields the relation-
ship sought between the power output of the source and the
space-time average sound pressure squared.

$$W_0 = \overline{p^2_{rev}} \left(\frac{S\bar{\alpha} + 4mV}{4\rho_0 c_0} \right) \qquad (4)$$

where V = room volume, m^2
      m = air absorption coefficient, m^{-1}

Cremer[1] gives the following approximation for the air absorption
factor at room temperature:

$$m = \frac{170}{(\beta)} (f)^2 \times 10^{-4} \qquad (5)$$

where m = absorption factor in $(meter)^{-1}$
      β = relative humidity in %
      f = frequency in kHz

The relation between the sound power output and the sound
pressure in the far field of an omnidirectional source in
distance, r, from the source's acoustical center is given by:

$$W_0 = \frac{[p(r)]^2 e^{mr} 4\pi r^2}{\rho_0 c_0} \qquad (6)$$

where p(r) = sound pressure at distance, r
      r = distance from the acoustical center of the source

10

In order to obtain a measure for the extent of the direct field for a source characterized by the directivity factor $Q(\gamma)$, it is customary to calculate the so-called "hall radius" which is the distance where the sound pressure of the direct field $p(r,\gamma)$ equals the space average sound pressure of the reverberant field, p_{rev}.

The hall radius, r_H, is obtained by equating Eq. 4 with Eq. 6 considering the equality of p_{rev} and $p(r,\gamma)$ and solving for r, yielding:

$$r_H = \sqrt{Q(\gamma)} \Big/ \sqrt{\frac{S\bar{\alpha} + 4mV}{16\pi}} \quad e^{-r_H m/2} \tag{7}$$

where $Q(\gamma)$ = directivity factor of radiation defined[2/] as the ratio of the sound intensity measured in direction, γ, to the sound intensity which would be measured at the same distance for an omnidirectional source of the same power output

The exponential term $e^{mr_H/2}$ in Eqs. 6 and 7, which takes into account the effect of air absorption on the direct sound wave does not differ much from unity even for the highest frequency of interest. Consequently, for our case we can neglect the exponential term in Eq. 7. Further considering the definition of the reverberation time:

$$T_R = \frac{0.163V}{S\bar{\alpha} + 4mV} \tag{8}$$

where V = room volume in m^3

$S\bar{\alpha}$ = total absorption in m^2

T_R = reverberation time in seconds :

The combination of Eqs. 7 and 8 yields the hall radius:

$$r_H \simeq 5.7 \times 10^{-2} \times \sqrt{Q(\gamma) \frac{V}{T_R}} \text{ , m} \tag{9}$$

where r_H = hall radius in meters

V = room volume in m^3

For the tunnel test section of $1.9 \times 10^4 m^3$ volume, equation 9 which is based on the assumption of a diffuse reverberant field would yield the following prediction formula for the hall radius in the test section:

$$r_H \simeq \frac{7.85\sqrt{Q(\gamma)}}{\sqrt{T_R}} \text{ , m} \tag{10}$$

Table I compares the hall radius values calculated from Eq. 10 by using the initial slope of the decay curve and assuming omnidirectional radiation [i.e. $Q(\gamma)=1$] with those evaluated from steady state measurements by **fitting** the standard SPL vs. distance curve of Fig. 5 to the measured data as shown schematically in Fig. 6. The hall radius so evaluated is plotted in Fig. 7 as a function of frequency.

TABLE I

COMPARISON OF THE CALCULATED AND MEASURED HALL RADIUS

f/Hz	31.5	63	125	250	500	1000	2000	4000	8000
T_R/sec	1.1	1.2	1.3	2.6	4.1	4.6	2.9	2.1	1.3
r_H/ft. calculated	24.1	23.3	22.2	15.9	12.7	11.9	15	17.5	22.2
r_H/ft. experimental	37	28	22	28	22	16	23	35	--

Observing the SPL vs. distance data for different directions
of the traverse, it was found that the hall radius did not
differ much in the various directions* so that the "experimental"
hall radius data given in Table I may be considered as repre-
sentative for all directions.

As can be seen from Table I the experimentally evaluated hall
radius values are generally much higher than the calculated
ones. This trend was expected to occur since, as already
pointed out in Section II, the sound energy radiated in the
direction of the shroud and nozzle openings contributes only
to the direct field but not at all to the reverberant field
of the test section. This then results in higher values of
the experimentally evaluated hall radius then one would expect
for a diffuse sound field. The non-diffuse nature of the
sound field in the test section violates our basic hypothesis
made in deriving Eq. 10 so that the calculated hall radius
values for a non-diffuse sound field are bound to be inaccurate.

In order to give an estimate for the approximate value of
the sound pressure level in the reverberant field of the test
section, which builds up if a steady state omnidirectional
source of known sound power output is elevated in the middle
of the test section, we have approximated the sound pressure
level in the reverberant field from the SPL vs. distance
curves, such as shown in Fig. 6. The reverberant sound pressure,
$\overline{SPL}_{REV}$, is found as the sound pressure level where the SPL
vs. distance curve levels off. After correcting these
$\overline{SPL}_{REV}$ values to correspond to 1 watt acoustical power of the
source, we obtained the so-called normalized reverberant
sound pressure levels given by Eq. 11:

---

*As expected, the traverses in the tunnel axis direction
 yielded a somewhat larger hall radius than the directions
 perpendicular to the tunnel axis. However, the difference
 was not larger than the overall accuracy of the measurements.

$$SPL_{N,REV} = \overline{SPL}_{REV} - PWL_o \qquad (11)$$

where $SPL_{N,REV}$ = the octave band reverberant sound pressure level normalized to 1 watt acoustical power output of the source

$\overline{SPL}_{REV}$ = the measured space-average octave band reverberant sound pressure level in dB re 0.0002μbar produced by an omnidirectional sound source of power level PWL_o

PWL_o = the known octave band sound power level of the omnidirectional source in dB re 10^{-12} watts

The expected octave band sound pressure level in the reverberant field of the test section produced by an omnidirectional sound source of the octave band sound power level PWL can then be approximated by:

$$\overline{SPL}_{REV} = SPL_{N,REV} + PWL \qquad (12)$$

where PWL = the sound power level of the omnidirectional source in dB re 10^{-12} watts

The normalized octave band reverberant sound pressure levels, $SPL_{N,REV}$, are given in Table II.

TABLE II
NORMALIZED OCTAVE BAND REVERBERANT SOUND PRESSURE LEVEL OF THE TUNNEL TEST SECTION

Octave Band Center Frequency in Hz	31.5	63	125	250	500	1000	2000	4000
$SPL_{N,REV}$ in dB	-33	-28	-29	-28	-27	-26	-30	-33

However, the normalized reverberant sound pressure level data
given in Table II should not be regarded as an acoustical
calibration of the test section which enables one to calculate
the sound power output of an unknown source by measuring and
inserting the space-average reverberant sound pressure level
into Eq. 10.

Equation 10 is valid only for an omnidirectional source suspended
at the center of the test stand. If the sound source has a
non-omnidirectional radiation pattern or is located at a
different position, Eq. 10 would result in a wrong estimate
of the power output of the unknown source.

V. DECAY RATE MEASUREMENTS

Because of the high ambient noise level in the tunnel, the
traditional ways of switching off a steady-state sound source
or bursting a balloon have not provided sufficient dynamic
range necessary for the proper evaluation of the decay curves.
Thus, a small 10 gauge cannon had to be used to yield the high
acoustical power output required.

As already discussed in Section II of this report, we expected
that the uneven spatial distribution of the sound absorbing
surfaces in the tunnel test section (i.e., the two large
openings of the shroud and nozzle at the upstream and down-
stream end) will cause an irregular, non-exponential decay
of the sound energy. An exponential decay would require a
diffuse sound field which is obviously not the case in the
tunnel test section.

The decay curves measured in the test section indeed show a
double slope as typified by the graph shown in Fig. 8. The
initial decay is controlled by those sound waves (rays)
which have a component in the direction of the tunnel axis
and, consequently, delivering energy to the shroud and nozzle
openings. After the energy of these waves is sufficiently
drained, the sound field in the test section and also the
tail-end of the decay curve is controlled by those waves
traveling in directions essentially perpendicular to the
tunnel axis. For these waves, which never hit the nozzle
and shroud openings, the rate of energy drainage and the
respective rates of decay are smaller than the decay of those
waves which control the initial part of the decay rate curve.

Since we were interested in evaluating how strongly the non-
diffuse character of the sound field manifests itself in
producing a difference between the hall radius values evaluated
from the spatial distribution of the sound field for steady
state excitation and those calculated from Eq. 10 by utilizing
the measured reverberation time and pretending that the
sound field was diffuse, we had to evaluate the "initial"
reverberation time. The "initial" reverberation times obtained
from the initial slope of the filtered decay rate curves
averaged from the recordings made at five different source
and receiver locations on the test platform are plotted in
Fig. 9. At low frequencies where the sound transmission loss
of the roof and the walls is low, the "initial" reverberation
time is in the order of 1 second. The highest reverberation
time of 4.6 seconds is reached in the 1000 Hz center frequency
octave band. Above 1000 Hz the effect of the air absorption
becomes noticeable and the reverberation time decreases
again with increasing frequency.

Other areas of the full scale wind tunnel provide one with
the opportunity to observe rare acoustical phenomena. Though
these phenomena are only of secondary interest for this study,
NASA may want to know about their existence in the full scale
wind tunnel.

For example, a very peculiar decay curve is recorded at the
mouth of the nozzle (location D in Fig. 1), where except for
those sound waves which are directed vertically and so remain
"trapped" between the parallel hard surfaces provided by the
ceiling and the floor, the sound waves with all other directions
experience hardly any reflections and can leave this section
of the tunnel through the nozzle or the acoustically transparent
turning vanes. Accordingly, after a very short and steep
decay, the sound field is constituted by a flutter echo between
the parallel ceiling and floor. The decay rate curve recorded
at this location is reproduced in Fig. 10. The pronounced
flutter can be heard for approximately 20 seconds.

Another interesting acoustical phenomenon was observed in the
return air corridors. Here, following an impulse type of
excitation, the corrugations of the tunnel walls act as
periodically spaced reflectors for the high frequency sound
and the observer experiences a feeling as if the sound would
come from a source which gradually climbs up the wall.

VI. ACOUSTICAL MEASUREMENTS IN THE TEST SECTION OF THE TUNNEL

The first necessary requirement to perform meaningful acoustical
measurements in the test section of the full scale wind tunnel
is that the sound pressure level produced by the test source
at the microphone location must exceed the level of the ambient
noise of the tunnel in the entire frequency region of interest.
The lowest possible ambient noise level is obtained when the
tunnel is stationary. This lowest ambient noise level should
be measured before starting each test run. The ambient noise
level with the tunnel operational can be predicted with sufficient
accuracy from Fig. 3 or Fig. 5. The extent of how much the
sound pressure of the test source at the microphone location
should exceed the ambient noise level depends on the sought
accuracy. To measure a signal with 1 dB accuracy the signal-to-
noise ratio should exceed 6 dB.

As discussed earlier, the reverberant sound field in the test
section of the tunnel is not diffuse. Accordingly, one cannot
find a generally valid relation between the space-average sound
pressure level in the test section and the sound power output
of an unknown sound source. Because of the concentration of
the sound absorbing boundaries (such as the nozzle and shroud
openings) at certain locations of the room boundaries, the
portion of the sound energy which will contribute to the
buildup of the reverberant field depends strongly on the direc-
tivity of the source (e.g., if most of the radiated energy is
directed toward these large openings, the sound pressure level
in the reverberant field will be much lower than in the case
when the source would radiate predominantly in the direction
of solid boundaries).

The approximate relation between the space-average reverberant
sound pressure level and the power level (given in Table II)
is valid only for omnidirectional sources suspended above the
center of the test platform. It is not valid for sound sources
with a directional radiation pattern.

In order to measure the total sound power output of an unknown
sound source located in the test section of the tunnel, one has
to measure the intensity of the direct sound field of the source
and integrate it over the entire surface of an imaginary enclosure
surrounding the source. In the far field of the source but well
within the hall radius, the sound intensity is proportional
to the sound pressure squared, namely:

$$I = \frac{p_{rms}^2}{\rho_0 c_0} \tag{13}$$

where p_{rms} = rms sound pressure level

ρ_0 = density of the air

c_0 = speed of sound in air

It is often convenient to measure the direct sound pressure
on the surface of an imaginary sphere of radius $r \ll r_H$ centered
on source location. In this case the total sound power output
of the source is obtained by integrating the squared rms pressure
over the total solid angle of 4π, namely:[3]

$$W_0 = \frac{r^2}{\rho_0 c_0} \int_{\xi=0}^{2\pi} \int_{0=0}^{\pi} p_{rms}^2(0,\xi,r)\sin 0 \, d0 \, d\phi \tag{14}$$

where $p_{rms}(0,\xi,r)$ = the rms sound pressure measured in distance,
r, from center of the source and in the
direction defined by the elevation angle 0
and polar angle ξ

In choosing the measuring distance r, one should be sure to be
in a range where the direct field dominates the reverberant
field. The hall radius as experimentally evaluated for an
omnidirectional source and plotted in Fig. 7 may serve as a
guide in selecting the proper radius. One should note, however,
that for a directive source the hall radius depends on the
directivity factor of the source so that in the direction of
maximum radiation the hall radius will be longer and in the mini-
mum direction shorter than the values obtained fo. an omni-
directional source. In order to measure the sound pressure level
of the direct sound with an accuracy of 1 dB, the measurement
distance should not exceed the half hall radius.

The non-diffuse character of the sound field in the tunnel test
section does not permit us to give a *quantitative* prediction for
the enlargement of the hall radius obtainable by providing a
certain amount of sound absorbing treatment for the presently
hard room boundaries. However, a *qualitative* estimate can be
made based on Eq. 9 by assuming that, at least,qualitatively, it
is also valid for a non-diffuse sound field. Equation 9 indicates
that an addition of sound absorbing treatment would enlarge the
hall radius by a factor approximately given by the square root
of the ratio of the average absorption co-efficient after and
before the treatment. Since the present average absorption
coefficient of the test section boundaries is in the order of
$\bar{\alpha} = 0.1$ in the frequency region from 500 Hz to 2000 Hz it may
well be possible to double the hall-radius in this frequency
range by covering certain presently hard surfaces with a rela-
tively thin (1 or 2 inches) layer of porous material such as
glass fiber, open cell acoustical foam or with a retractable
flannel curtain of proper flow-resistance. The sound absorbing
treatment should cover those hard room boundaries which have a
line of sight from the location of the test object.

A quantitative evaluation of the effectiveness of a sound
absorbing wall treatment in respect of enlarging the hall-
radius should be determined in a small-scale acoustical
model (i.e. scale 1:20) of the tunnel test section where the
tunnel openings are represented by completely abosrbing
surfaces. In gradually adding sound absorbing treatment to
the various hard interior surfaces the optimal location and
the minimum amount of the sound absorbing material required
to yield a desired result can be determined.

The optimum combination of the amount and location of the sound
absorbing treatment determined in the model would assure that
the sound absorbing treatment in the full-scale test section is
designed in a balanced manner yielding maximum improvement for
the invested funds.

REFERENCES

1. Cremer, L., STATISTISCHE RAUMAKUSTIK, S. Hirzel, Stuttgart, 1961, p. 27.

2. Beranek, L.L., ed., NOISE REDUCTION, McGraw-Hill Book Company, Inc., New York, 1960, p. 165.

3. Beranek, L.L., ACOUSTICS, McGraw-Hill Book Company, Inc., New York, 1954, p. 109.
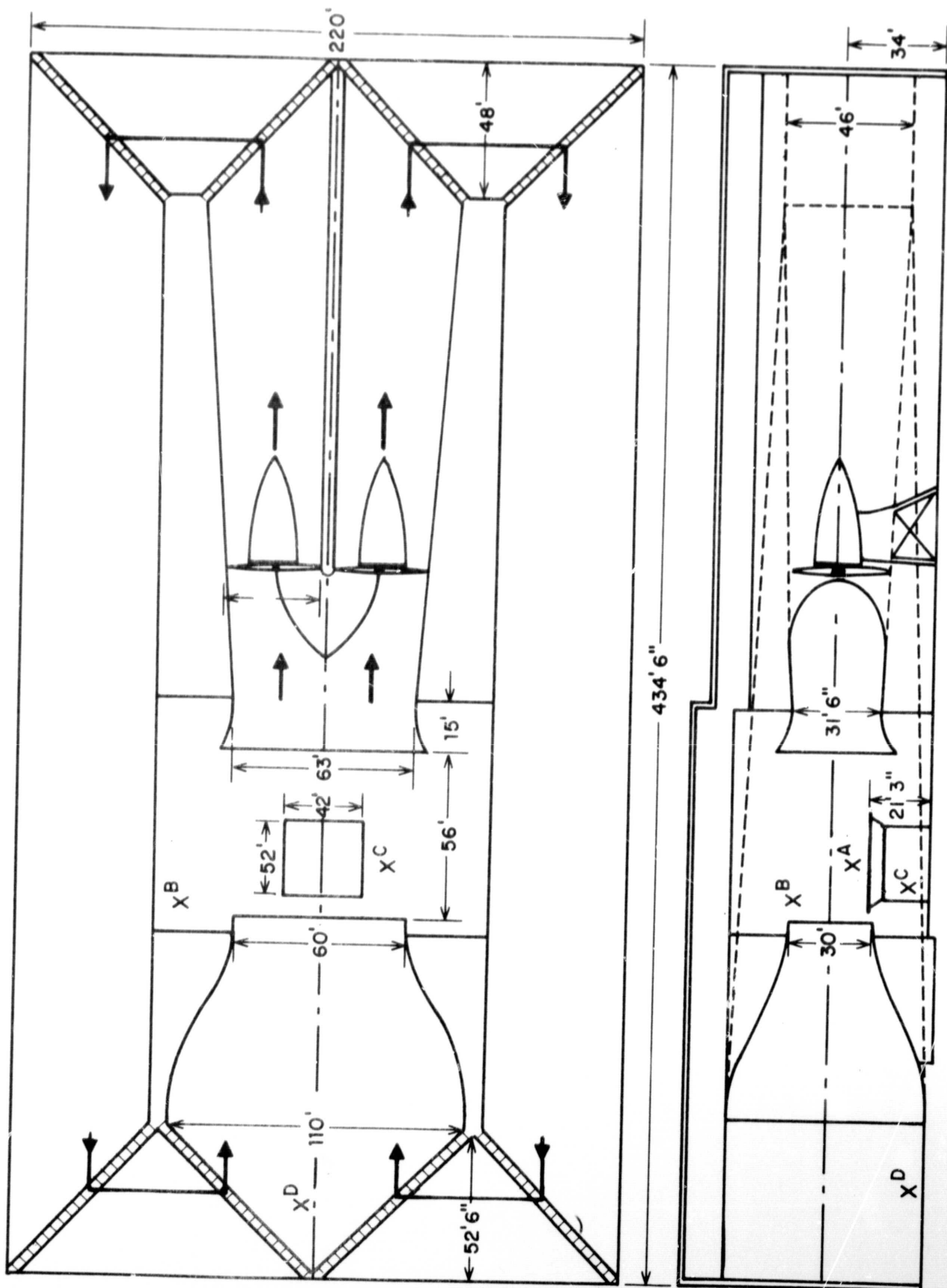
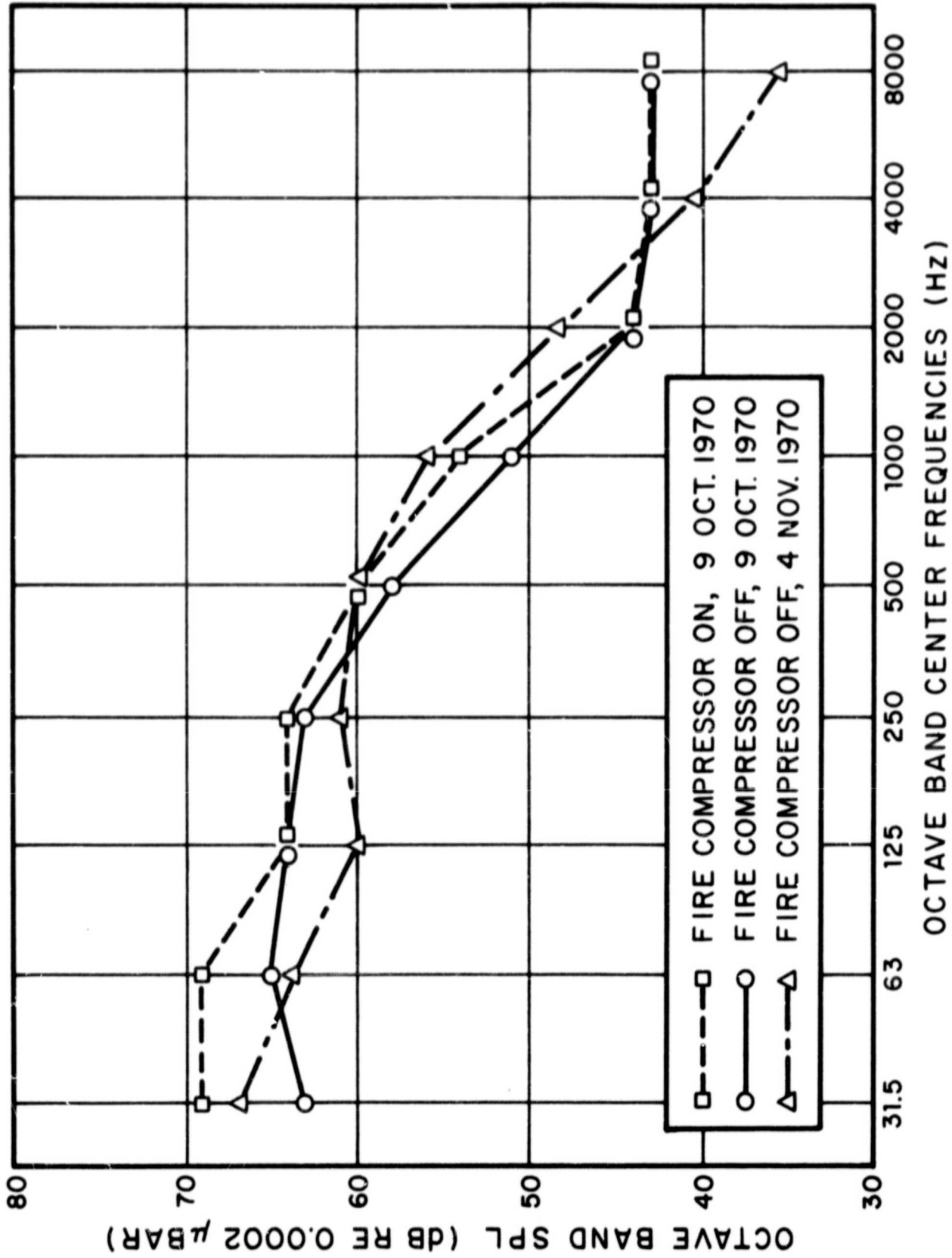FIG. 1　PLAN AND CROSS-SECTION OF THE TUNNEL

FIG. 2   OCTAVE BAND AMBIENT NOISE LEVEL ON THE TEST PLATFORM, TUNNEL STATIONARY
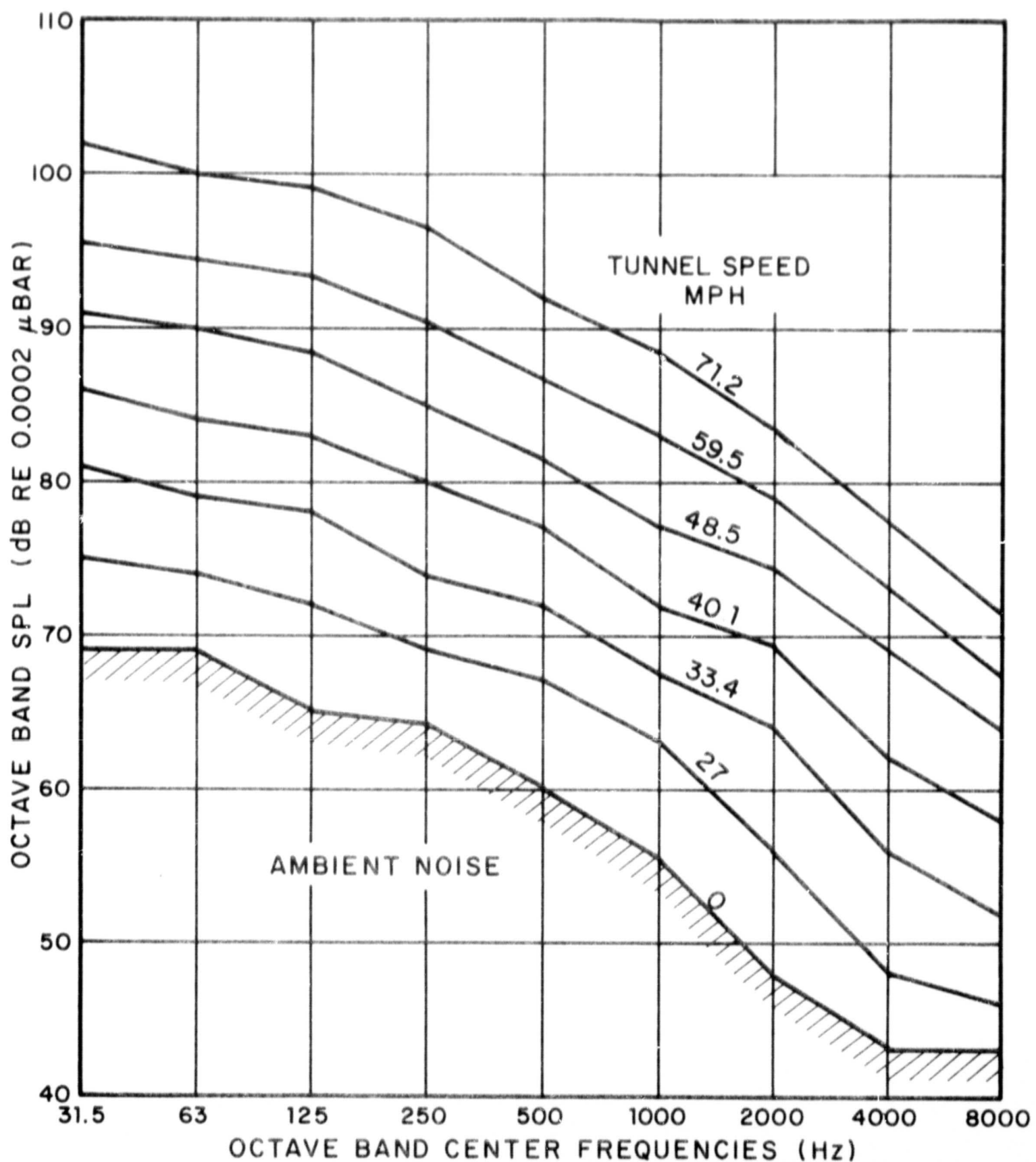
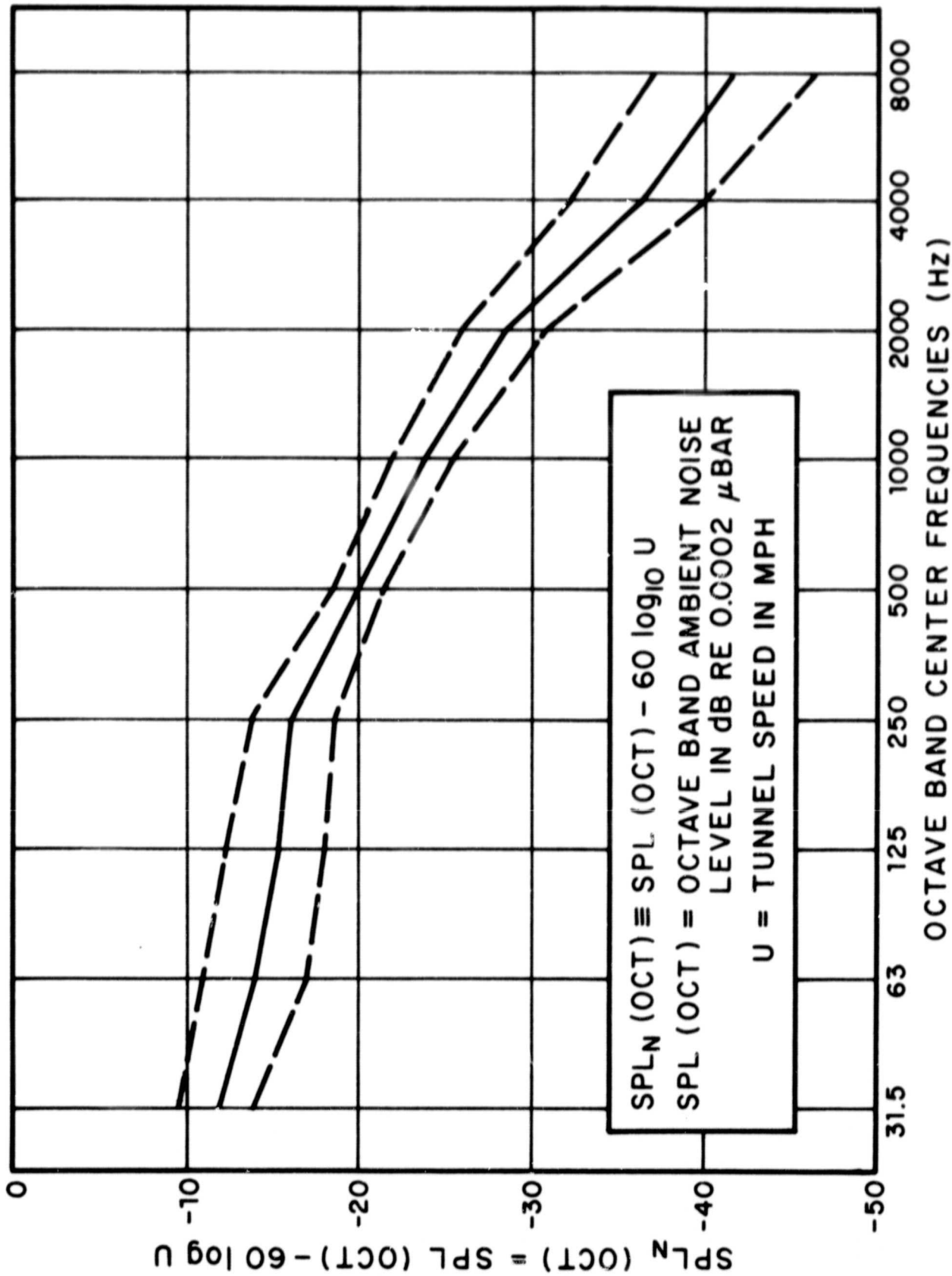FIG. 3   OCTAVE BAND AMBIENT NOISE LEVEL ON THE TEST PLATFORM
         (POSITION A) WITH TUNNEL SPEED AS PARAMETER

SPL$_N$ (OCT) $\equiv$ SPL (OCT) - 60 log$_{10}$ U

SPL (OCT) = OCTAVE BAND AMBIENT NOISE
            LEVEL IN dB RE 0.0002 μBAR

U = TUNNEL SPEED IN MPH

OCTAVE BAND CENTER FREQUENCIES (Hz)

SPL$_N$ (OCT) = SPL (OCT) - 60 log U

FIG. 4   RANGE OF NORMALIZED OCTAVE BAND AMBIENT NOISE LEVELS
          FOR MICROPHONE POSITIONS A, B, AND C, TUNNEL SPEED
          RANGE 27MPH-71MPH
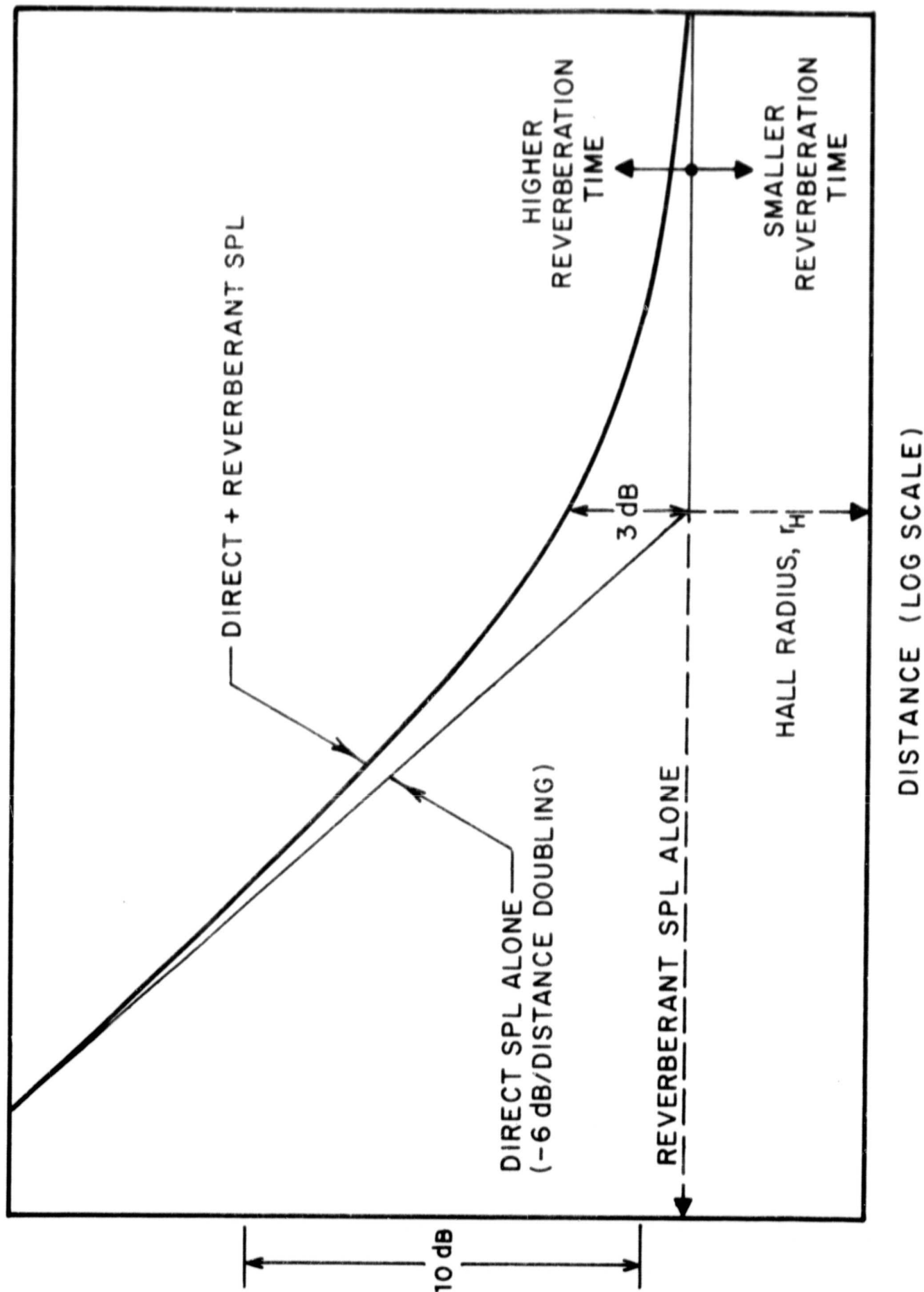
FIG. 5   SPL VS DISTANCE FOR AN OMNIDIRECTIONAL SOUND SOURCE
          RADIATING INTO A ROOM
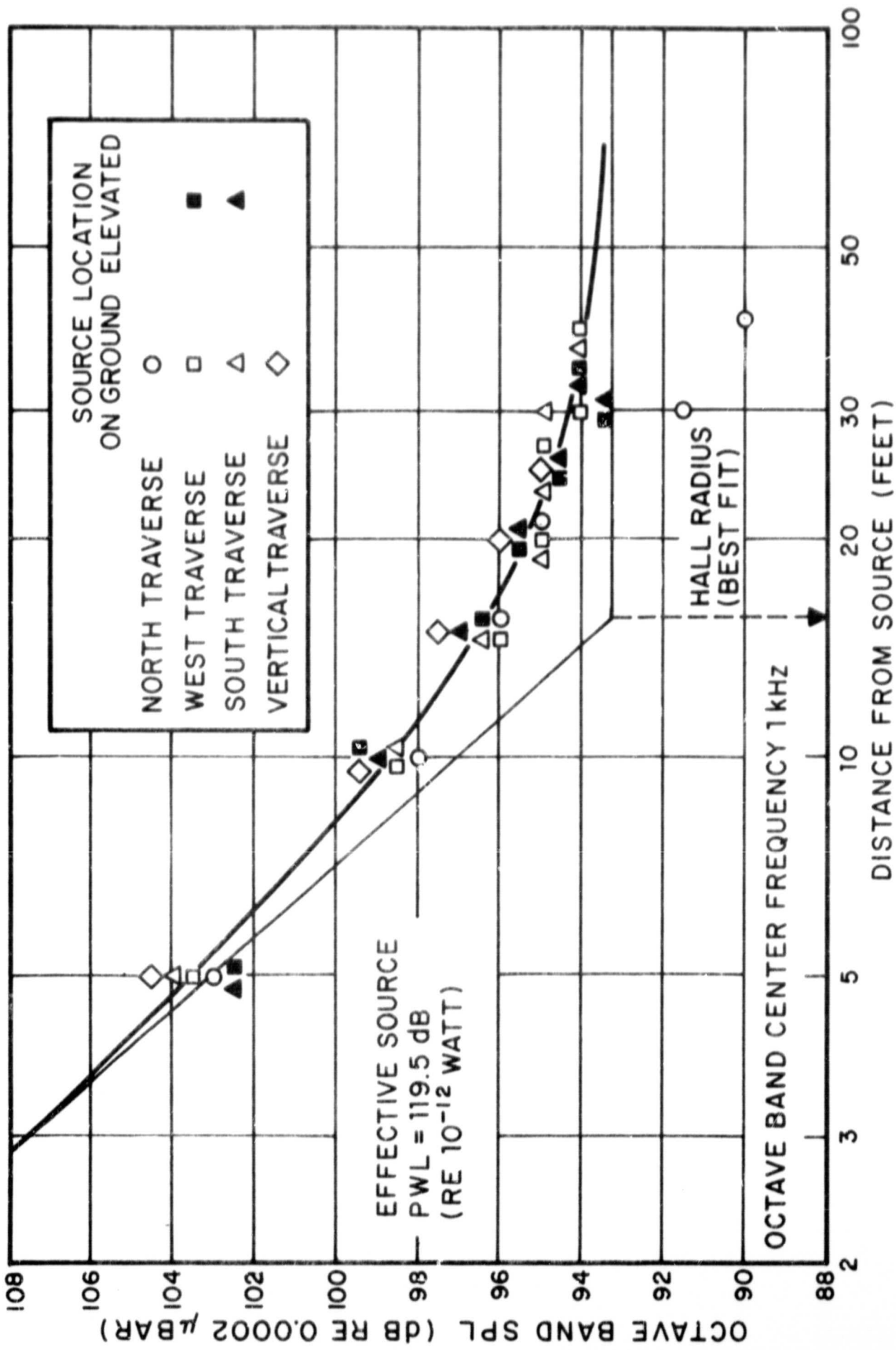
FIG. 6   EXAMPLE FOR THE EVALUATION OF THE "HALL-RADIUS", r_H, FROM THE EXPERIMENTAL DATA
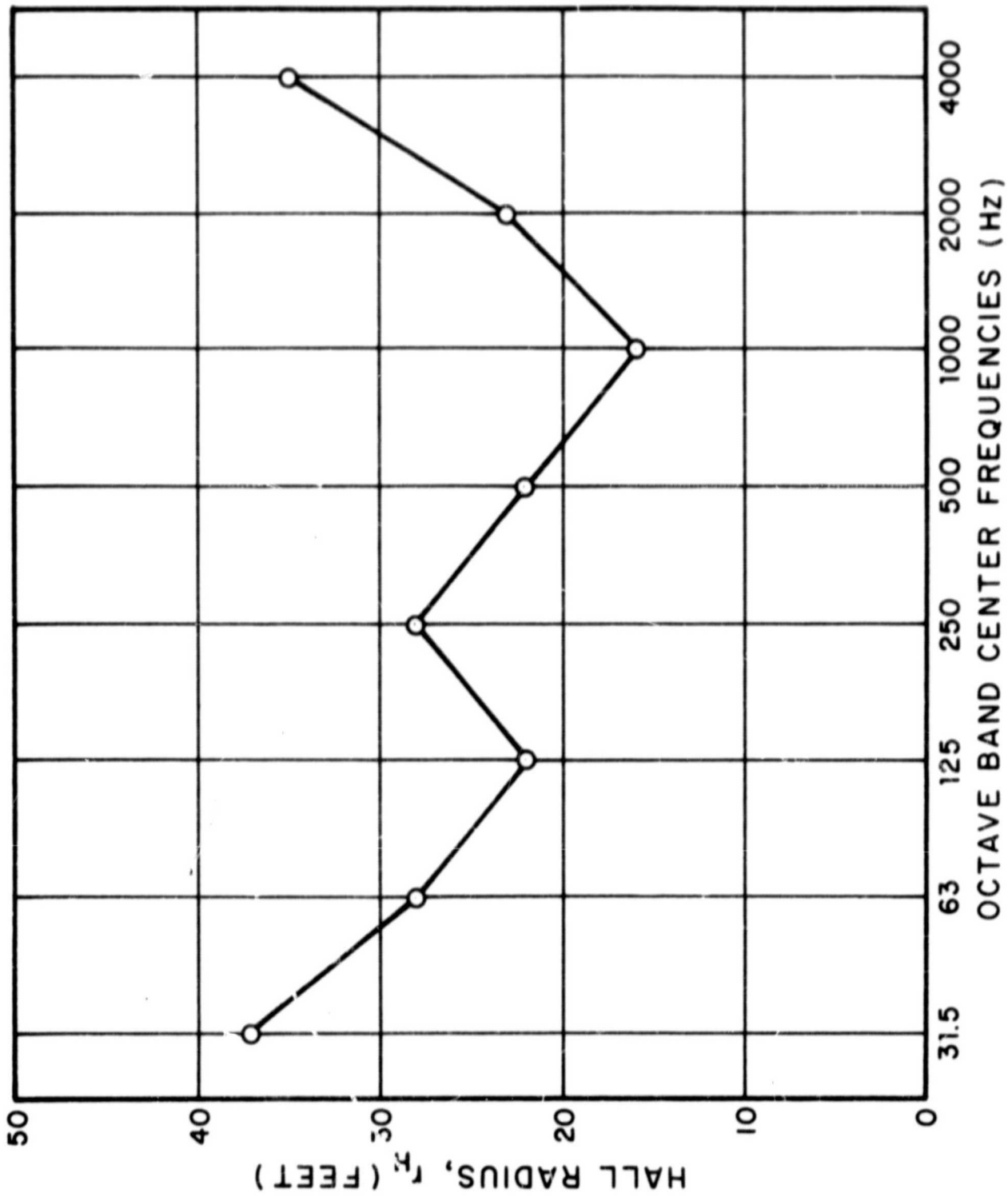
FIG. 7   HALL RADIUS, r_H, EVALUATED FROM MEASURED SPL VS DISTANCE CURVES (BEST FIT)
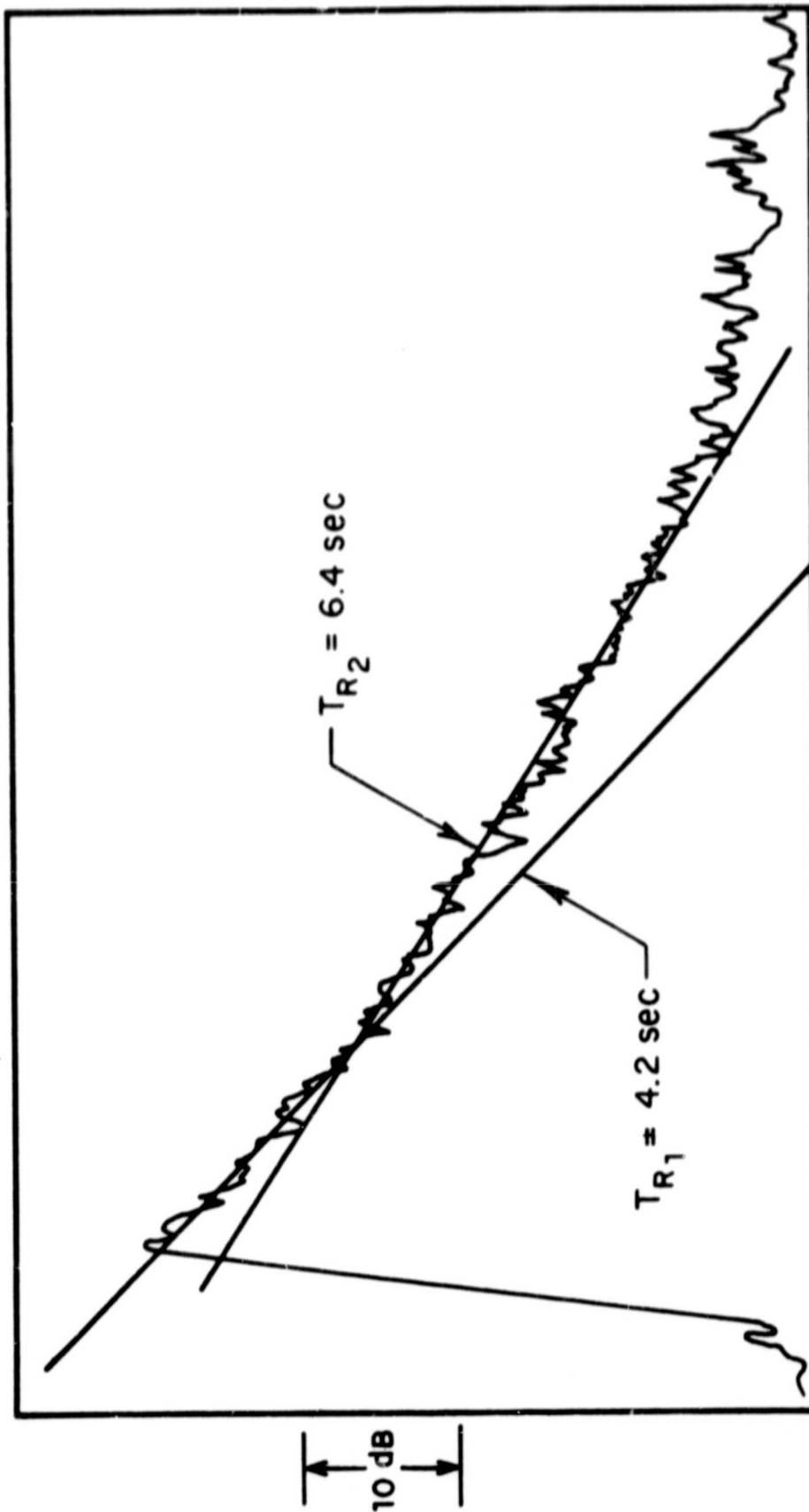
FIG. 8   TYPICAL DOUBLE-SLOPED DECAY CURVE OBTAINED ON THE
         TEST PLATFORM:
         OCTAVE BAND CENTER FREQUENCY 1 kHz
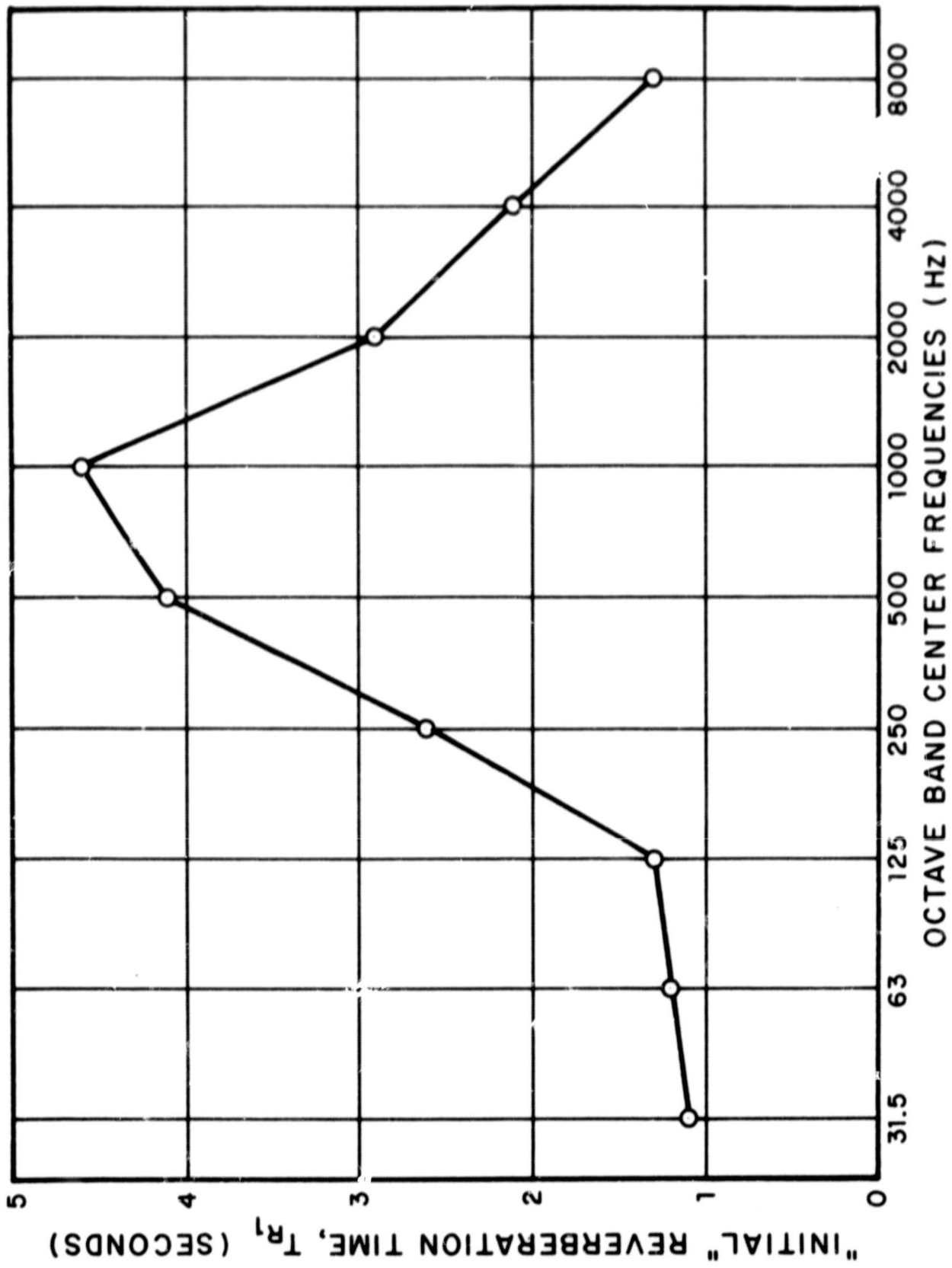   PAPER SPEED 30 mm/sec
         PEN SPEED 200 mm/sec

OCTAVE BAND CENTER FREQUENCIES (Hz)

FIG. 9   INITIAL REVERBERATION TIME, T_{R_1}, EVALUATED FROM THE
INITIAL SLOPE OF THE DECAY CURVE MEASURED IN THE TEST
SECTION (AVERAGE OF 5 SOURCE AND RECEIVER LOCATIONS)
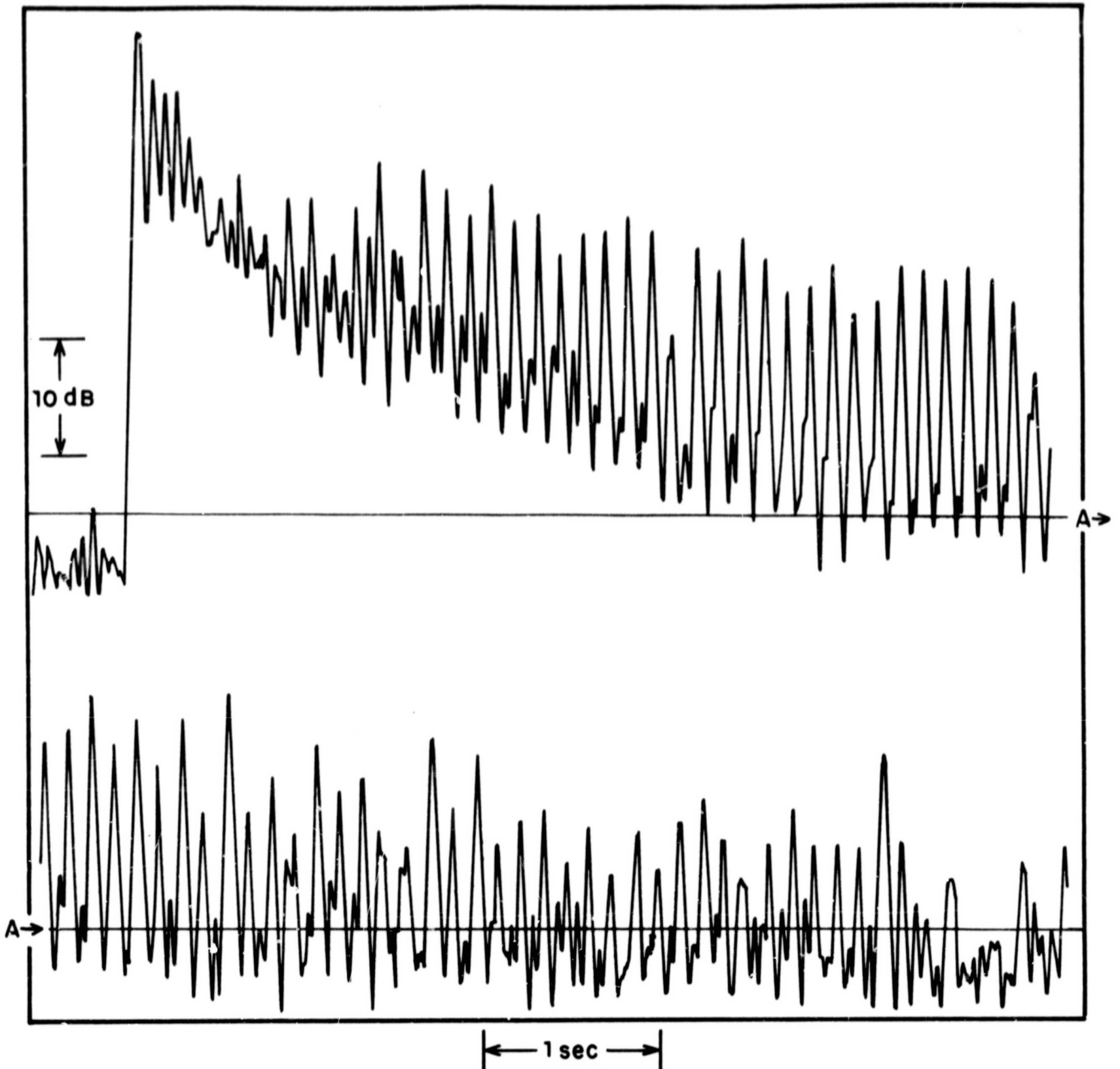
FIG. 10   OVERALL DECAY CURVE MEASURED IN POSITION "D" SHOWING
            UNUSUALLY STRONG FLUTTER ECHO
            PAPER SPEED 30 mm/sec
            PEN SPEED 1000mm/sec